JOURNAL OF MATERIALS SCIENCE 31 (1996) 371–379

Measuring the elastic properties of high-modulus fibres

P. J. HINE, I. M. WARD
IRC in Polymer Science and Technology, University of Leeds, Leeds LS2 9JT, UK

The measurement of the elastic constants of several highly oriented thermoplastic polymer fibres is described. The method makes use of the hot-compaction process, developed and patented in this laboratory, which enables a solid section of highly oriented polymer to be produced from an aggregate of highly oriented fibres. As only a small fraction of the original fibre is melted and recrystallized during the process, the compacted materials offer a unique opportunity for measuring fibre properties in the bulk. An ultrasonic immersion technique is used to measure the elastic properties of the compacted materials, from which the properties of the polymer fibres are inferred. The experimentally determined fibre elastic properties have been compared with other oriented polymer materials to assess any similarities in elastic anisotropy between different methods for producing fibre orientation, and compared with theoretical upper limits for the fibre elastic properties based on theoretical estimates for the polymer crystal unit cell appropriately averaged for hexagonal symmetry using the aggregate model.

1. Introduction

A complete description of the elastic properties of a drawn high-modulus polymer fibre is seldom available, for although it is relatively simple to measure the longitudinal and torsional moduli, it is extremely difficult to measure the transverse modulus and Poisson's ratios of a fibre that is sometimes only tens of micrometres in diameter. Methods do exist for measuring transverse properties of fibres, for instance the transverse compression test, and a number of authors have used this method to determine the transverse properties of, for instance, polyethylene fibres. Even when this measurement is possible, there is still a considerable advantage in having a method which measures a full set of elastic constants for a fibre under the same conditions of temperature and frequency.

The uses for a full set of elastic constants for an oriented polymer fibre are numerous. It enables a fuller understanding of the role of the polymer microstructure on the elastic properties of the fibre to be investigated, through the use of theoretical simulations. It allows similarities in elastic anisotropy with other oriented polymer systems to be explored, including large-scale oriented products such as die-drawn and extruded materials and fibre-reinforced composites. Finally, a full description of the elastic properties of a fibre provides a vital starting point for modelling work on fibre-reinforced composite materials. While outside the scope of this current paper, this is an area of study which has so far shown considerable predictive success through our work on glass, carbon and polyethylene fibre-reinforced epoxy composites [1–4].

A method is described here for determining a full set of elastic constants for a number of thermoplastic polymer fibres, utilizing the technique of hot compaction. In this process, developed in this laboratory and patented by The British Technology Group (GB Patent 2253420), fibres are compacted together under suitable conditions of temperature and pressure to form a homogeneous material in which a major fraction of the original fibre is retained [5–9]. The advantage of the compaction technique is that it provides a sample of substantial size on which a set of consistent measurements can easily be made, while giving a high retention of the properties of the original fibre: this makes it ideal for estimating the properties of the original fibre.

The measurement of the elastic properties of five different fibre types (melt-spun polyethylene, gel-spun polyethylene, polypropylene, polyethylene terephthalate and a thermotropic liquid crystalline polymer) is reported. The technique used for measuring the fibre elastic constants was the ultrasonic immersion method, originally implemented by Read and Dean at NPL [10] and further developed by Lord [11, 12] and Woolf [13]. This technique gives a full set of elastic constants, all determined at the same frequency and temperature. Once determined, the fibre elastic constants were used for a number of interesting calculations and comparisons, some of which we allude to above.

2. Experimental procedure

2.1. Hot compaction

The basis of this work is the hot compaction process, where high modulus, small diameter, polymer fibres

0022–2461

are compacted to form thick section homogeneous products [5–9]. The details of five fibres used in this study are shown in Table I. The compaction process for the five fibres was basically the same. Firstly the fibres were wound around a C-shaped former, of separation 65 mm, and placed into a matched metal mould of area 55 mm × 55 mm: enough fibre was wound around the former to ensure a final product of approximately 3 mm thickness. The mould was then placed into a hot press, which was set to the compaction temperature for the particular fibre (as shown in Table I). A light pressure of 100 p.s.i. (10^3 p.s.i. $= 6.89\ N\,mm^{-2}$) was then applied while the fibre/mould assembly heated up. Once the mould reached the compaction temperature it was left for a further 10 min and then a high pressure of 3000 p.s.i. was applied for 10 s. The mould was then cooled and the sample removed. Slight variations in the process were required for each individual fibre while following the above basic formula. For instance, the gel-spun polyethylene fibres required a higher pressure during the initial phase of the process (160 p.s.i.) because of a higher shrinkage stress developed by the fibres close to their melting range.

In the majority of the fibres, the compaction process works by "selectively melting" a small proportion of the fibres' surface during the original low-pressure phase. Application of the high pressure consolidates the product, removing air and any excess molten material. On cooling, the molten portion reforms (in some cases recrystallizes) to bind the structure together. Only the gel-spun polyethylene fibre failed to show any significant surface melting [14]. However, the compaction process on this fibre does produce a reasonable level of fibre-to-fibre adhesion which results in a homogeneous product on which measurements can be made.

It will be appreciated that a range of compaction temperatures are possible for each fibre, trading off the fibre properties, which fall with the amount of fibre melted, with transverse strength, which rises with the amount of fibre melted. In this work, where transverse strength is of less importance, we have chosen compaction temperatures that are the lowest that give perfect compaction, allowing maximum retention of fibre properties which can then be measured. For a close-packed hexagonal arrangement of circular fibres, only 9% of the melted and recrystallized phase is needed to fill all the gaps in the structure, and this is the proportion aimed at with the samples made for this work, using the temperatures shown in Table I.

A typical transverse section, in this case through a compacted melt-spun polyethylene sample, is shown in Fig. 1, etched to give contrast between the different morphologies: this picture was taken by Professor Bassett and his colleagues at the University of Reading. The spaces in between the closed-packed fibres are seen to be filled with melted and reformed material. The holes seen within each fibre are due to internal defects which preferentially etch out. While the mechanism of compaction may differ between the five fibre types, the essential point is that the compacted material contains a consolidated aligned assembly of the respective fibres, with a substantial percentage of the original fibre remaining. Fuller details of the compaction process, typical mechanical properties, and details of internal morphology can be found elsewhere for the melt-spun polyethylene [5–8] and for polyethylene terephthalate [9]. Details of the compacted gel-spun polyethylene [14] and the polypropylene will appear shortly.

TABLE I Details of the fibres and the compaction temperatures

Fibre type	Company	Grade	Compaction temperature (°C)
Melt-spun polyethylene	SNIA fibre	Tenfor	138
Gel-spun polyethylene	DSM	Dyneema	145
Polyethylene terephthalate	ICI	Tyre cord Yarn (38035 T800)	256
Polypropylene	F. Drake and Co.	Leonene	164
Thermotropic liquid crystal polymer	Hoechst Celanese	Vectran	280

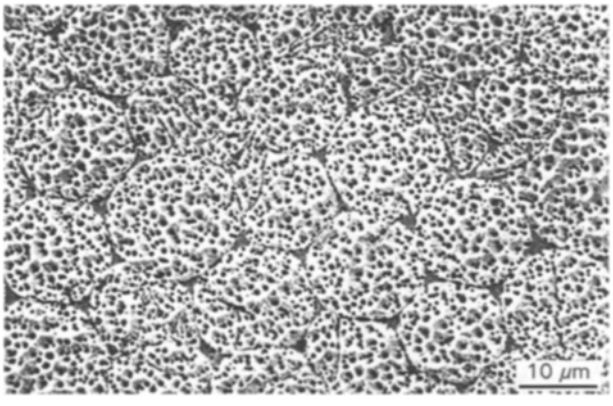

Figure 1 A transverse section from a compacted melt-spun polyethylene fibre sample.

2.2. Measurement of elastic properties

The elastic properties of the compacted materials were determined using the ultrasonic velocity method [10–13]. The sample to be measured is placed in a water bath (at 25 °C) between two ultrasonic transducers (2.25 MHz), one acting as a transmitter and one acting as a receiver. The basic measurement is the time of flight for a sound pulse to travel between the transducers. When the sample is at right angles to the beam, only a tensile wave is propagated through the sample. However, as the sample is rotated away from the normal, a shear wave is generated at the front surface of the sample.

Two equations exist which relate the shape of the velocity of the tensile, V_t, and shear waves, V_s, with angle of refraction, r, to the elastic properties of the sample in the plane of propagation of the wave. Defining the three major axes of the samples to be 1, 2 and 3,

if the wave is propagating in the 23 plane then these equations are given as

$$V_t = \frac{B_{22} + B_{33} + [(B_{22} - B_{33}) + 4B_{23}^2]^{1/2}}{2\rho} \quad (1)$$

for tensile waves, and

$$V_s = \frac{B_{22} + B_{33} - [(B_{22} - B_{33}) + 4B_{23}^2]^{1/2}}{2\rho} \quad (2)$$

for shear waves, where

$$B_{22} = C_{22}\cos^2(r) + C_{44}\sin^2(r) \quad (3a)$$

$$B_{33} = C_{33}\sin^2(r) + C_{44}\cos^2(r) \quad (3b)$$

$$B_{23} = (C_{44} + C_{23})\sin(r)\cos(r) \quad (3c)$$

and ρ is the sample density and C_{ij} are the sample stiffness constants. Similar equations can be written for sound propagation in the 13 and 12 planes.

Measurements of the pulse transit time, for both the tensile and shear waves, are taken over a range of incidence angles, allowing the tensile and shear-wave velocities with refraction angle to be calculated. A computer program is then used to determine the best fit to the experimental points using the above two equations, which results in best estimates for the four elastic constants C_{33}, C_{22}, C_{23} and C_{44}. This experiment is shown schematically in Fig. 2a, where we define the 3 axis of the sample as the fibre direction, the 1 axis of the sample perpendicular to the 3 axis in the plane of the sheet, and the 2 axis as out of plane. The sound wave propagates in the 23 plane and the sample is rotated around the 1 axis.

If the sample is rotated about the 2 axis by 90°, and the experiment is repeated, then the same procedure will yield the elastic constants C_{11}, C_{22}, C_{66} and C_{12} (Fig. 2b). As will be shown in Section 3, these two experiments yield all the elastic constants necessary for a full description of the properties of the compacted plates, and hence the fibres.

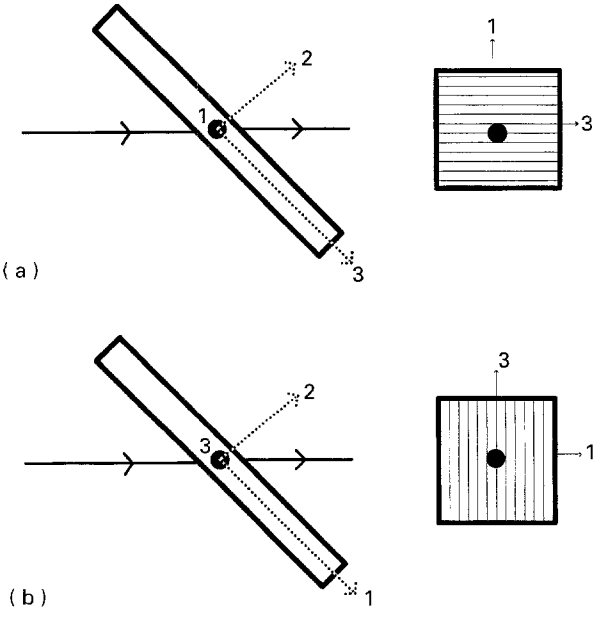

Figure 2 The two ultrasonic experiments needed to obtain a full set of elastic constants: (a) $C_{33}, C_{22}, C_{44}, C_{23}$, (b) $C_{11}, C_{22}, C_{66}, C_{12}$.

3. Theory

The anisotropic elastic behaviour of an oriented material is described by the generalized Hooke's law as

$$\varepsilon_i = S_{ij}\sigma_j \quad \text{where } i, j = 1, \ldots, 6 \quad (4a)$$

$$\sigma_i = C_{ij}\varepsilon_j \quad (4b)$$

These two equations relate applied stresses, σ_j, and applied strains, ε_j, to measured strains, ε_i, and measured stresses, σ_i, through the compliance constants, S_{ij}, and the stiffness constants, C_{ij}. These relationships can be expanded into a series of equations of the form

$$\sigma_1 = C_{11}\varepsilon_1 + C_{12}\varepsilon_2 + C_{13}\varepsilon_3 + C_{14}\varepsilon_4 + C_{15}\varepsilon_5 + C_{16}\varepsilon_6 \quad (5)$$

$$\sigma_2 = \ldots, \sigma_3, = \ldots, \text{etc.}$$

or more conveniently expressed in matrix form as

$$\begin{bmatrix}\sigma_1\\ \sigma_2\\ \sigma_3\\ \sigma_4\\ \sigma_5\\ \sigma_6\end{bmatrix} = \begin{bmatrix}C_{11} & C_{12} & C_{13} & C_{14} & C_{15} & C_{16}\\ C_{21} & C_{22} & C_{23} & C_{24} & C_{25} & C_{26}\\ C_{31} & C_{32} & C_{33} & C_{34} & C_{35} & C_{36}\\ C_{41} & C_{42} & C_{43} & C_{44} & C_{45} & C_{46}\\ C_{51} & C_{52} & C_{53} & C_{54} & C_{55} & C_{56}\\ C_{61} & C_{62} & C_{63} & C_{64} & C_{65} & C_{66}\end{bmatrix}\begin{bmatrix}\varepsilon_1\\ \varepsilon_2\\ \varepsilon_3\\ \varepsilon_4\\ \varepsilon_5\\ \varepsilon_6\end{bmatrix} \quad (6)$$

A similar matrix can be written for the compliance constants S_{ij}.

In the most general case, 36 constants are needed to describe completely the elastic properties of a material. Under conditions of symmetry the number of independent constants rapidly diminishes. The compacted materials concerned here all show transverse isotropy, sometimes described as fibre symmetry. The symmetry axis in this system is the 3 axis, and is defined as the main fibre direction, while the other two axes, 1 and 2, form an isotropic plane. For this system there are only five independent elastic constants shown by the matrix below.

$$\begin{bmatrix}\sigma_1\\ \sigma_2\\ \sigma_3\\ \sigma_4\\ \sigma_5\\ \sigma_6\end{bmatrix} = \begin{bmatrix}C_{11} & C_{12} & C_{13} & 0 & 0 & 0\\ C_{12} & C_{11} & C_{13} & 0 & 0 & 0\\ C_{13} & C_{13} & C_{33} & 0 & 0 & 0\\ 0 & 0 & 0 & C_{44} & 0 & 0\\ 0 & 0 & 0 & 0 & C_{44} & 0\\ 0 & 0 & 0 & 0 & 0 & 2(C_{11} - C_{12})\end{bmatrix}\begin{bmatrix}\varepsilon_1\\ \varepsilon_2\\ \varepsilon_3\\ \varepsilon_4\\ \varepsilon_5\\ \varepsilon_6\end{bmatrix} \quad (7)$$

The two ultrasonic experiments described above in the experimental section, and shown schematically in Fig. 2, are therefore all that is necessary to determine all the constants, C_{ij}, of the compacted plates. Once the stiffness matrix is determined, a matrix inversion is used to determine the compliance constants, S_{ij}. The engineering constants can then be determined from

the usual relationships: the longitudinal modulus $E_{33} = 1/S_{33}$; the transverse modulus, $E_{11} = 1/S_{11}$; the Poisson's ratios, $\nu_{13} = -S_{13}/S_{33}$ and $\nu_{12} = -S_{12}/S_{11}$, and finally the shear modulus, $G_{13} = C_{44}$.

4. Results

4.1. Ultrasonic immersion method

A typical set of results, of tensile and shear-wave velocities against angle of refraction, r, for compacted melt-spun polyethylene fibre, is shown in Fig. 3. The solid symbols indicate the experimentally measured points, while the dotted lines show the computer best fit to the curve shapes: in both cases the top curve indicates the tensile wave while the bottom curve is the shear wave. Fig. 3a shows the velocity angle relationship for sound propagating in the 23 plane while rotating the sample about the 1 axis (as defined in Fig. 2a). Fig. 3b shows the velocity angle relationship for sound propagating in the 12 plane and rotating the sample about the 3 axis (as defined in Fig. 2b). It is clear from Fig. 3b that both the tensile and shear-wave velocities are independent of the angle of refraction for this second sample orientation, confirming the 12 plane to be isotropic, and therefore the material as transversely isotropic. This was true for all five compacted samples. A full set of results, for the five compacted fibre types, is shown in Tables II and III. Table II shows stiffness constants, C_{ij}, while Table III shows the engineering constants.

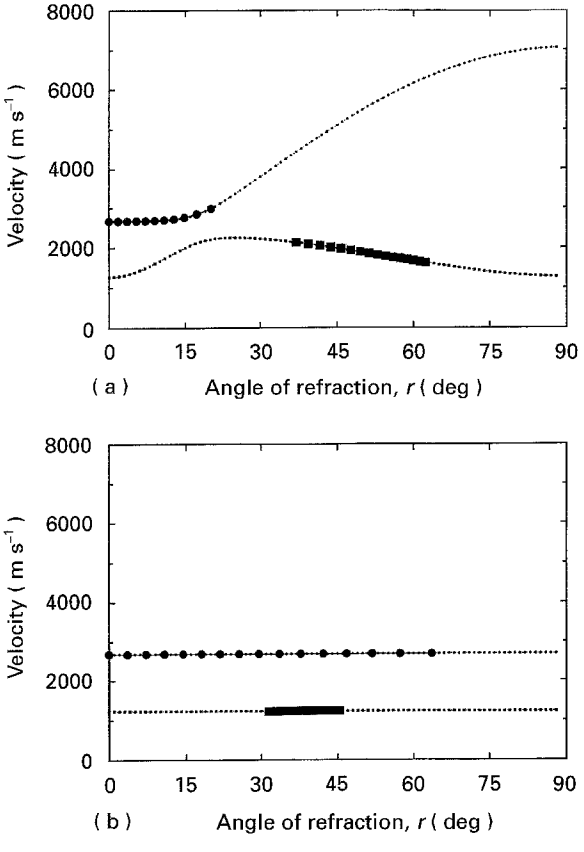

Figure 3 A typical set of results of (a) the tensile velocity, V_l, and (b) the shear velocity, V_s, plotted against the angle of refraction, r. (●, ■) The experimental measurements: (···) theoretical best fits to the data.

TABLE II The measured stiffness constants of the compacted plates/fibres

Fibre type	C_{33} (GPa)	C_{11} (GPa)	C_{13} (GPa)	C_{12} (GPa)	C_{44} (GPa)
Tenfor	62.3	7.16	5.09	4.15	1.63
Dyneema	79.1	6.69	5.03	3.94	1.36
PET	18.8	7.70	5.07	5.45	1.62
PP	12.8	4.11	2.50	2.58	1.55
LCP	103.1	7.33	6.12	5.46	1.30

C_{33}, C_{11}, C_{12} and C_{44} ± 2%: C_{13} ± 5%.

TABLE III The elastic properties of the compacted plates/fibres

Fibre type	E_{33} (GPa)	E_{11} (GPa)	ν_{13}	ν_{12}	G_{13} (GPa)
Tenfor	57.7	4.68	0.45	0.55	1.63
Dyneema	74.3	4.31	0.47	0.57	1.36
PET	14.9	3.70	0.39	0.65	1.62
PP	11.0	2.41	0.39	0.58	1.52
LCP	97.2	3.24	0.48	0.73	1.30

E_{33} ± 3%, all others ± 2%.

Before discussing the results in detail, it is worth considering possible sources of error in these measurements. The work of many authors, most recently that of Clarke *et al.* [3], have shown that although the method of fitting Equations 1 and 2 to the velocity/angle data can determine most of the elastic constants to within 1% error, it can produce errors in the shear stiffnesses (e.g. C_{13}) of up to 10%. Certainly repeated measurements on a single material in this work (e.g. Fig. 4) showed a scatter of over 5% for C_{13}, while the other constants were very repeatable. Tables II and III indicate typical errors in the measured constants.

The nature of the compacted material, as an arrangement of fibres within a melted and reformed phase, leads to two other sources of error in extrapolating the measured elastic properties of the original fibres from measurements on the compacted materials. Firstly the fibres may not be perfectly aligned along the nominal fibre direction, leading to a low estimate for the longitudinal fibre stiffness, C_{33}. Secondly the compacted material is, in effect, a composite with the melted and reformed material reinforced by the original fibres. Therefore, all the measured compacted material properties will be a combination of the properties of the two phases. The effect of this can be investigated by choosing one fibre, the melt-spun polyethylene, and making measurements on a range of samples with different fibre volume fractions, achieved by compacting the fibre over a range of temperatures within the melting range. Fig. 4 shows the results of these experiments: Fig. 4a shows all five elastic constants plotted against the fraction of the melted and reformed phase, while Fig. 4b shows more detail of the four lower value constants. It is seen that the value of C_{33} changes rapidly with fibre volume fraction, while the other four constants are relatively independent of volume fraction. Extrapolating back to 0% matrix fraction gives estimates of 100% fibre properties:

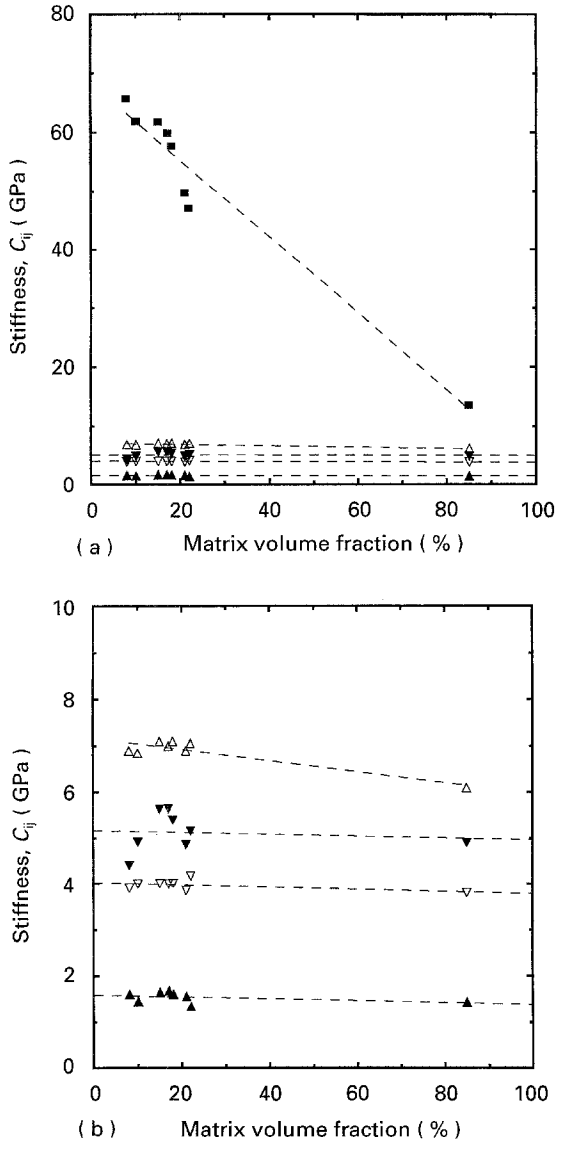

Figure 4 Stiffness constants for compacted melt-spun polyethylene fibres for a range of matrix volume fractions. (a) (■) C_{33}, (Δ) C_{11}, (▼) C_{13}, (▽) C_{12}, (▲) C_{44}. (b) (Δ) C_{11}, (▼) C_{13}, (▽) C_{12}, (▲) C_{44}.

TABLE IV A comparison of the stiffness constants of the melt-spun polyethylene fibre, determined from a sample compacted at 138 °C and from extrapolating to 100% fibre

	C_{33} (GPa)	C_{11} (GPa)	C_{13} (GPa)	C_{12} (GPa)	C_{44} (GPa)
Compacted at 138 °C	62.3	7.16	5.09	4.15	1.63
Extrapolated to 100% fibre	68.5	7.17	5.16	4.02	1.59

C_{33}, C_{11}, C_{12} and C_{44} ± 2%: C_{13} ± 5%.

a comparison between this extrapolation and the results for the lowest matrix volume fraction obtainable from the compaction process (8%), are shown in Table IV. It is seen that taking the values from the highest volume fraction of fibre leads to a 10% low estimate of C_{33}, but excellent estimates for the other four constants. (C_{33} is likely to be even lower due to the effects of misorientation as discussed above.) We can therefore conclude that the estimated fibre values of C_{33} and E_{33}, obtained from the compacted samples, are likely to be between 10% and 20% too low, while the other four constants should be an excellent estimate of the fibre values. For any detailed modelling work, utilizing fibre constants obtained using this technique, it is obviously necessary to carry out measurements over a range of fibre volume fractions and extrapolate to 100% fibre volume fraction. Time does not allow such a range of experiments to be carried out here, for all the five fibre types involved in this study, so that the results shown in Tables II and III and the rest of this paper, refer to measurements on the highest fibre volume fraction possible using the compaction technique.

5. Discussion

5.1. General discussion

The results for the elastic constants are collated in Tables II and III and show a marked similarity in terms of the elastic anisotropy. It is well known that the longitudinal stiffness C_{33} (or E_{33}) is generally much larger in value than the other elastic constants, because this relates to intramolecular bond stretching and bond bending rather than intermolecular dispersion forces. Values of C_{33} in the range of 100 GPa for the polyethylene and liquid crystalline polymer (LCP) fibres can be understood in terms of the very high degrees of molecular orientation achieved in their processing, together with the comparatively straight molecular chains. The lower value of C_{33} for polyethylene terephthalate (PET) and polypropylene (PP) relate to different factors, the lower degree of molecular orientation in the case of PET and the helical structure of the molecular chain in PP (together with a comparatively modest degree of molecular orientation). What is more surprising is the close similarity in absolute terms for the values of C_{11}, C_{12}, C_{13} and C_{14} and the corresponding engineering elastic constants E_{11}, ν_{12}, ν_{13} and G_{13}. The only exceptions to this are the three stiffness constants C_{11}, C_{12} and C_{13} for the polypropylene fibre which show values around half of those measured for the other four fibres.

It is particularly interesting to note that whereas in all cases ν_{13} is less than 0.5, ν_{12} is invariably greater than 0.5. The liquid crystalline fibre, Vectran, shows the greatest degree of anisotropy with the highest longitudinal modulus, E_{33}, a low transverse modulus, E_{11}, the lowest shear modulus, G_{13}, and very high anisotropy in the Poisson's ratios. As discussed in detail elsewhere [15], this pattern of anisotropy is consistent with an "ideal" fibre-reinforced material, where a matrix with a very low shear modulus is reinforced by very stiff fibres. The Poisson's ratio ν_{13} is ≈ 0.5 which shows that there is only a small volume contraction for stress applied along the 3 direction (the chain-axis direction). On the other hand, $\nu_{12} \approx 0.7$ (and $\nu_{23} \approx 0$) implies that application of stress in the 2 direction causes almost no deformation in the 3 direction, with all the deformation accommodated by pure shear in the 12 plane. To the approximation that $\nu_{12} \approx 1$, it can readily be shown that $G_{12} = 1/4\ E_{11}$.

For this Vectran fibre, G_{12} was measured at 0.831 GPa, predicting a value for E_{11} of 3.32 GPa which compares very well indeed with the measured value of 3.24 GPa.

5.2. Comparison with other oriented polymers

The ultrasonic results for compacted fibres are compared with those for die-drawn rods of Rigidex 50 polyethylene (draw ratio 20) [16] and PPH 6065 polypropylene (draw ratio 10.5) [17] in Tables V and VI, respectively. The polyethylene data, measured at 10 MHz by Leung *et al.*, are in close agreement and confirm that the compaction procedure is very effective indeed in producing bulk specimens with the elastic properties of highly oriented fibres. It would be expected that the value of E_{33} for the fibre should be much larger than the die-drawn sheet as the fibres have a much higher draw ratio. This confirms the problem of underestimating the value of E_{33} using the compaction method as described above in Section 4. Although the results for polypropylene, measured at 10 MHz by Chan *et al.* [17] are not in quite such close agreement with regard to C_{12} and C_{13}, all the other elastic constants are close in value and it can again be concluded that the compaction technique has been applied satisfactorily. Both of these comparisons confirm that the elastic anisotropy of the drawn fibres and the bulk drawn thick section sheets is virtually identical.

A further comparison of this nature is shown in Table VII for the Vectran LCP fibre and an injection-moulded plate of a different thermotropic liquid crystalline polymer [18]. Although the compacted fibres and the injection-moulded plaques are not identical in chemical structure (Vectran is 70:30 *p*-hydroxybenzoic acid/*p*-hydroxynaphthoic acid, whereas SRP1 is 36:32:32 *p*-hydroxybenzoic acid/isophthalic acid/hydroquinone) the elastic anisotropy is very similar indeed. In the compacted fibres, E_{33} is much greater than for the moulded plaque, owing to the higher molecular orientation, but the other elastic constants appear to be little affected either by molecular orientation, as previously concluded, or more interestingly by detailed chemical structure.

TABLE V A comparison of the stiffness constants of the melt-spun fibre (Tenfor) and die-drawn polyethylene sheet

Process	C_{33} (GPa)	C_{11} (GPa)	C_{13} (GPa)	C_{12} (GPa)	C_{44} (GPa)
Compacted, (Tenfor) C_{33}, C_{11}, C_{12} and $C_{44} \pm 2\%$: $C_{13} \pm 5\%$	62.3	7.16	5.09	4.15	1.63
Die-drawn DR = 20	66.0	6.90	4.40	3.90	1.60

TABLE VI A comparison of the stiffness constants of the polypropylene (PP) fibre and die-drawn sheet

Process	C_{33} (GPa)	C_{11} (GPa)	C_{13} (GPa)	C_{12} (GPa)	C_{44} (GPa)
Compacted (PP) C_{33}, C_{11}, C_{12} and $C_{44} \pm 2\%$: $C_{13} \pm 5\%$	16.2	4.86	2.85	2.65	1.67
Die-drawn PP (DR = 10.5)	15.0	4.16	1.7	1.15	1.98

TABLE VII A comparison of the propertes of the compacted fibre (Vectran) and injection-moulded plates (SRP1) for a thermotropic liquid crystalline polymer

Process	E_{33} (GPa)	E_{11} (GPa)	ν_{13}	ν_{12}	G_{13} (GPa)
Compacted (Vectran) $E_{33} \pm 3\%$, all others $\pm 2\%$	97.2	3.24	0.48	0.73	1.30
Injection-moulded SRP1	15.6	2.92	0.50	0.71	1.43

5.3. Comparison with fibre-reinforced composites

Table VIII shows a comparison between the stiffness constants of compacted melt-spun polyethylene fibre and a melt-spun polyethylene fibre epoxy/ composite with 55% fibre content. It can be seen that there is again remarkable agreement in the elastic anisotropy of the two materials. This result is of importance in two respects. First, it is clear that the compacted fibres offer a route to obtaining comparable elastic properties to those of conventional fibre/resin composites, but with great advantages for recycling and other environmental issues. Secondly, this result confirms our view of the structures of the polyethylene fibres, where we have proposed that they are akin to a short fibre composite with long crystals acting as reinforcing fibres.

Further support for this viewpoint comes from two other sources. First, there are the results for the thermotropic liquid crystalline polymers, where we have seen that the actual chemical structure of the chain molecules is of secondary importance in determining the elastic anisotropy. Secondly, as discussed above, the actual pattern of anisotropy in the oriented liquid crystalline polymer is consistent with an "ideal" fibre-reinforced composite material. In particular, we have already observed a remarkable anisotropy in the Poisson's' ratios. Much more detail of the comparison between the properties of compacted polyethylene fibre composites, die-drawn polyethylene fibre/epoxy composites can be found elsewhere [4].

5.4. Theoretical estimates of fibre elastic constants

A comparison was made of the experimental results obtained from the compacted materials with theoretical

TABLE VIII A comparison of the stiffness constants of the compacted melt-spun polyethylene fibre and a melt-spun polyethylene fibre/epoxy composite (55% fibre volume fraction)

Process	C_{33} (GPa)	C_{11} (GPa)	C_{13} (GPa)	C_{12} (GPa)	C_{13} (GPa)
Compacted PE	62.3	7.16	5.09	4.15	1.63
PE/epoxy composite	54.8	7.62	5.89	4.39	1.71

C_{33}, C_{11}, C_{12} and $C_{44} \pm 2\%$: $C_{13} \pm 5\%$.

calculations of the fibre elastic constants. This was carried out for polyethylene and polypropylene.

5.4.1. Polyethylene

The crystal structure of polyethylene is of orthorhombic symmetry so that the elastic behaviour is specified by nine independent elastic constants. The stiffness matrix is given by

$$\begin{bmatrix} C_{11} & C_{12} & C_{13} & 0 & 0 & 0 \\ C_{12} & C_{22} & C_{23} & 0 & 0 & 0 \\ C_{13} & C_{23} & C_{33} & 0 & 0 & 0 \\ 0 & 0 & 0 & C_{44} & 0 & 0 \\ 0 & 0 & 0 & 0 & C_{55} & 0 \\ 0 & 0 & 0 & 0 & 0 & C_{66} \end{bmatrix} \quad (9)$$

where the principal axes of the elastic anisotropy are chosen for simplicity to coincide with the a, b and c axes of the orthorhombic unit cell.

The compacted samples which have been examined in this research are all of fibre symmetry. To make a comparison between experiment and theory it is therefore necessary to estimate the theoretical predictions for a polyethylene sample of hexagonal symmetry. This can be done as the basis of the aggregate model [19], assuming that the sample consists of a transversely isotropic aggregate of orthorhombic units averaging the unit cell elastic constants in the plane normal to the c axis (chain axis) direction. The averaging can be done either in terms of stiffness constants (Voigt average) or compliance constants (Reuss average). These two averaging schemes represent upper and lower bounds to the elastic constants. For the stiffness constants the aggregate model gives the elastic constants of the equivalent fibre C'_{11}, C'_{12}, C'_{13}, C'_{33} and C'_{44} as

$$C'_{11} = C'_{22} = \frac{3}{8}C_{11} + \frac{3}{8}C_{22} + \frac{1}{4}C_{12} + \frac{1}{2}C_{66} \quad (10a)$$

$$C'_{12} = \frac{1}{8}C_{11} + \frac{1}{8}C_{22} + \frac{3}{4}C_{12} - \frac{1}{2}C_{66} \quad (10b)$$

$$C'_{13} = \frac{1}{2}(C_{13} + C_{23}) \quad (10c)$$

$$C'_{33} = C_{33} \quad (10d)$$

and

$$C_{44} = \frac{1}{2}(C_{44} + C_{55}) \quad (10e)$$

where C_{ij} are the constants of the polyethylene crystal cell. Similar equations for S'_{11}, S'_{12}, etc., with only two changes: in the equation for S'_{11} the last term is (1/8) S_{66} while for S'_{12} the last term is $-(1/8)\ S_{66}$.

The elastic constants for the polyethylene crystal unit cell structure have been calculated by many researchers, including Odajima and Maeda [20], Tashiro *et al.* [21], Karasawa *et al.* [22], Sorensen *et al.* [23], and more recently Lacks and Rutledge [24]. In essence the theoretical estimates are arrived at by a knowledge of the unit-cell dimensions and the intermolecular force constants. Sophisticated computer-modelling packages are now available which allow this form of simulation to be relatively easily performed. The difference in the theoretical estimates, from the various authors, lies partly in the temperature of the prediction (often at 0 K), and partly in the values of the off-diagonal stiffnesses C_{12}, C_{13} and C_{23}. These particular stiffness constants are very sensitive to such factors as the unit cell dimensions which affect the intermolecular force fields, which are themselves very sensitive to the detailed assumptions made in the calculations.

We have attempted to examine the various stiffness calculations for polyethylene in comparison with our experimental data. Some of the predicted stiffness matrices, notably those by Karasawa *et al.* and Sorensen *et al.*, were found not to satisfy required strain-energy criteria and it was therefore not possible to calculate the compliance constants for our comparison between theory and experiment. The best correlation between theory and experiment came from the work of Lacks and Rutledge [24]. These authors have used the force field of Karasawa *et al.* but included the effect of thermal motions, enabling the calculation of the properties of the crystal over a range of temperatures from 0–400 K. For our comparison the most appropriate values are those at 300 K.

In Table IX we show the stiffness constants, C_{ij}, for crystalline polyethylene calculated by Lacks and Rutledge with those calculated for fibre of equivalent structure on the Voigt and Reuss averaging schemes, together with our ultrasonic results for compacted fibres (the Voigt and Reuss bounds were very close for most of the stiffness constants and so we show the mean of the upper and lower bounds in Table IX). It can be seen that the measured pattern of anisotropy corresponds very well with that predicted theoretically, including good prediction of the off diagonal constants. The value of C_{33} is much greater than any of the other values because deformation in the fibre axis direction involves stretching and bending of extended chain molecules. The lower value of the experimentally measured C_{33} compared with the theoretical prediction can be attributed partly to lack of perfect overall orientation, and partly due to the limited crystal length in the fibres. It has been proposed in several alternative models for the structure of these fibres that the extended chains in long crystalline sequences

TABLE IX A comparison of measured fibre properties and theoretical predictions for polyethylene

Crystal unit stiffness constants (300 K) (GPa) Lacks and Rutledge [24]

$$\begin{bmatrix} 8.8 & 4.3 & 4.5 & 0 & 0 & 0 \\ 4.3 & 8.8 & 5.8 & 0 & 0 & 0 \\ 4.5 & 5.5 & 290 & 0 & 0 & 0 \\ 0 & 0 & 0 & 3.4 & 0 & 0 \\ 0 & 0 & 0 & 0 & 2.4 & 0 \\ 0 & 0 & 0 & 0 & 0 & 3.0 \end{bmatrix}$$

Calculated equivalent fibre (average of Reuss and Voigt) (GPa)

$$\begin{bmatrix} 9.15 & 3.95 & 5.15 & 0 & 0 & 0 \\ 3.95 & 9.15 & 5.15 & 0 & 0 & 0 \\ 5.15 & 5.15 & 290 & 0 & 0 & 0 \\ 0 & 0 & 0 & 2.86 & 0 & 0 \\ 0 & 0 & 0 & 0 & 2.86 & 0 \\ 0 & 0 & 0 & 0 & 0 & 2.6 \end{bmatrix}$$ 9

Compacted fibre properties (GPa)

$$\begin{bmatrix} 7.16 & 4.15 & 5.09 & 0 & 0 & 0 \\ 4.15 & 7.16 & 5.09 & 0 & 0 & 0 \\ 5.09 & 5.09 & 62.3 & 0 & 0 & 0 \\ 0 & 0 & 0 & 1.63 & 0 & 0 \\ 0 & 0 & 0 & 0 & 1.63 & 0 \\ 0 & 0 & 0 & 0 & 0 & 1.57 \end{bmatrix}$$

TABLE X A comparison of measured fibre properties and theoretical predictions for polypropylene

Crystal unit stiffness constants (300 K) (GPa) Tashiro *et al.* [21]

$$\begin{bmatrix} 7.78 & 3.91 & 3.72 & 0 & 0.90 & 0 \\ 3.91 & 11.55 & 3.99 & 0 & -0.36 & 0 \\ 3.72 & 3.99 & 42.44 & 0 & -0.57 & 0 \\ 0 & 0 & 0 & 4.02 & 0 & -0.12 \\ 0.90 & -0.36 & -0.57 & 0 & 3.10 & 0 \\ 0 & 0 & 0 & -0.12 & 0 & 2.99 \end{bmatrix}$$

Calculated equivalent fibre (average of Reuss and Voigt) (GPa)

$$\begin{bmatrix} 9.53 & 3.73 & 3.83 & 0 & 0 & 0 \\ 3.73 & 9.53 & 3.83 & 0 & 0 & 0 \\ 3.83 & 3.83 & 42.4 & 0 & 0 & 0 \\ 0 & 0 & 0 & 3.53 & 0 & 0 \\ 0 & 0 & 0 & 0 & 3.53 & 0 \\ 0 & 0 & 0 & 0 & 0 & 2.90 \end{bmatrix}$$

Compacted fibre properties (GPa)

$$\begin{bmatrix} 4.11 & 2.58 & 2.50 & 0 & 0 & 0 \\ 2.58 & 4.11 & 2.50 & 0 & 0 & 0 \\ 2.50 & 2.50 & 12.8 & 0 & 0 & 0 \\ 0 & 0 & 0 & 1.55 & 0 & 0 \\ 0 & 0 & 0 & 0 & 1.55 & 0 \\ 0 & 0 & 0 & 0 & 0 & 0.80 \end{bmatrix}$$

reinforce the structure in a similar manner to the fibres in a short-fibre composite, so that there is a shear-lag effect which reduces the modulus due to the finite aspect ratio of the reinforcing crystalline elements [25].

5.4.2. Polypropylene

The crystal structure of polypropylene is monoclinic, so that a number of the other elements in the stiffness matrix of the crystal unit become non-zero (see Table X). However the equations for predicting the

equivalent fibre elastic constants, using the aggregate model, reduce to the same as shown above for polyethylene (Equations 10a–e). The elastic constants for the polypropylene monoclinic unit cell are not currently available from Lacks and Rutledge so we have used the alternative estimates of Tashiro *et al.* [21], determined at 0 K. Comparison between the ultrasonic data for compacted fibres and theoretical calculation, again using the aggregate model to give the equivalent fibre, are shown in Table X. As for polyethylene, it appears that the pattern of mechanical anisotropy is similar to that measured, but in this case the actual measured values are all systematically lower than those predicted by Tashiro *et al.* For C_{33} this can be attributed to the lower degree of molecular orientation in the fibres compared to the perfect crystal, but in the case of the other elastic constants, it is likely that this is partly due to the calculation being for low temperatures, and partly due to the fact that there is a substantial contribution from amorphous material which has a much lower stiffness.

6. Conclusion

The compaction technique offers an excellent route to obtaining all the elastic constants for a range of thermoplastic fibres, by providing a thick section material with comparable elastic properties to the original fibres on which ultrasonic measurements can be carried out. It is concluded that the value of C_{33}, determined from the compacted materials, is an underestimate of the fibre properties, owing to imperfect fibre orientation and the effect of the melted and recrystallized phase. The other four stiffness constants, C_{11}, C_{12}, C_{13} and C_{44}, are less affected by these factors and can be estimated with a high degree of confidence. Even more interestingly, these latter four constants are broadly similar for the five different fibre types, indicating that they are comparatively insensitive to chemical structure and molecular orientation. This was confirmed by a comparison between a compacted LCP fibre, and an injection-moulded LCP of different chemical structure and orientation: the four constants were again very similar. The LCP fibre results were also of interest in showing the greatest level of elastic anisotropy, with, in particular, the Poisson's ratios ν_{13} and ν_{12} approaching the theoretical limits of 0.5 and 1.0, respectively, for an "ideal" fibre-reinforced material.

The elastic anisotropy of the fibres was compared with other oriented polymer materials, notably die drawn rods and polymer/epoxy composites. In all cases the elastic anisotropy was very similar for these different classes of materials, emphasizing that the compact on process offers an alternative route to useful oriented products.

Finally, the measured elastic constants were used as an end point for comparing with theoretical simulations of the fibre properties, based on the properties of the polymer crystal cell. Excellent agreement was obtained between the theoretical and experimental stiffness constants for polyethylene and reasonable agreement was seen for polypropylene.

References

1. P. J. HINE, R. A. DUCKETT and I. M. WARD, *Compos. Sci. Technol.* **49** (1993) 13.
2. X. GONG, P. J. HINE, R. A. DUCKETT and I. M. WARD, *Polym. Compos.* **15** (1994) 74.
3. J. F. CLARKE, R. A. DUCKETT, P. J. HINE and I. M. WARD, *Composites* **25** (1994) 863.
4. O. DARRAS, P. J. HINE, R. A. DUCKETT and I. M. WARD, *Compos. Sci. Technol.* in press.
5. P. J. HINE, I. M. WARD, R. OLLEY and D. C. BASSETT, *J. Mater. Sci.* **28** (1993) 316.
6. R. OLLEY, D. C. BASSETT, P. J. HINE and I. M. WARD, *ibid.* **28** (1993) 1107.
7. M. A. KABEEL, D. C. BASSETT, R. H. OLLEY, P. J. HINE and I. M. WARD, *ibid.*, **29** (1994) 4694.
8. *Idem, ibid.* **30** (1995) 601.
9. J. RASBURN, P. J. HINE, I. M. WARD, R. H. OLLEY, D. C. BASSETT and M. A. KABEEL, *ibid.*
10. B. E. READ and G. D. DEAN, "The determination of the dynamic properties of polymers and composites" (Adam Hilger, Bristol, 1978) p. 162.
11. D. LORD, PhD thesis, University of Leeds (1989).
12. S. R. A. DYER, D. LORD, I. J. HUTCHINSON, I. M. WARD and R. A. DUCKETT, *J. Phys. D Appl. Phys.* **25** (1992) 66.
13. A. WOOLF, *Polym. Test.* **5** (1985) 375.
14. J. RASBURN, "The compaction of gel spun polyethylene", Internal Report (1993).
15. D. L. GREEN, G. R. DAVIES and I. M. WARD *Polymer* in press.
16. W. P. LEUNG, F. C. CHEN, C. L. CHOY, A. RICHARDSON and I. M. WARD, *Polymer* **25** (1984) 447.
17. O. K. CHAN, F. C. CHEN, C. L. CHOY and I. M. WARD, *J. Phys. D Appl. Phys.* **11** (1978) 617.
18. J. SWEENEY, B. BREW, R. A. DUCKETT and I. M. WARD, *Polymer* **33** (1992) 4901.
19. I. M. WARD, *Proc. Phys. Soc.* **80** (1962) 1176.
20. A. ODAJIMA and M. MAEDA, *J. Polym. Sci.* **19** (1979) 1023.
21. K. TASHIRO, M. KOBAYASHI and H. TADOKORO, *Macromolecules* **11** (1978) 914.
22. N. KARASAWA, S. DASGUPTA and W. A. GODDARD, *J. Phys. Chem.* **95** (1991) 2260.
23. R. A. SORENSEN, W. B. LIAU, L. KESNER and R. H. BOYD, *Macromolecules* **21** (1988) 200.
24. D. J. LACKS and G. C. RUTLEDGE, *J. Phys. Chem.*, **98** (1994) 1222.
25. I. M. WARD, "Mechanical properties of solid polymers", 2nd Edn (Wiley, 1983) p. 314.

Received 1 October 1994
and accepted 9 January 1995